Liquid Crystals

Publication details, including instructions for authors and subscription information:
http://www.informaworld.com/smpp/title~content=t713926090

Antiferroelectric alignment and mechanical director rotation in a hydrogen-bonded chiral SmC^*_A elastomer

Alexei S. Merekalov; Sergei A. Kuptsov; Georgii A. Shandryuk; Raisa V. Talroze; Vladimir S. Bezborodov; Eugene M. Terentjev

To cite this Article Merekalov, Alexei S. , Kuptsov, Sergei A. , Shandryuk, Georgii A. , Talroze, Raisa V. , Bezborodov, Vladimir S. and Terentjev, Eugene M.(2001) 'Antiferroelectric alignment and mechanical director rotation in a hydrogen-bonded chiral SmC^*_A elastomer', Liquid Crystals, 28: 4, 495 — 502

To link to this Article: DOI: 10.1080/02678290010017953

URL: http://dx.doi.org/10.1080/02678290010017953

Liquid Crystals, 2001, Vol. 28, No. 4, 495–502

Antiferroelectric alignment and mechanical director rotation in a hydrogen-bonded chiral SmC$_A^*$ elastomer

ALEXEI S. MEREKALOV, SERGEI A. KUPTSOV,
GEORGII A. SHANDRYUK, RAISA V. TALROZE*
A. V. Topchiev Institute of Petrochemical Synthesis, Russian Academy of Sciences,
Leninsky pr. 29, Moscow 117912, Russia

VLADIMIR S. BEZBORODOV
A. N. Shevchenko Institute for Applied Physics, Kurchatova st. 7,
Minsk 220064, Belarus

and EUGENE M. TERENTJEV
Cavendish Laboratory, University of Cambridge, Cambridge CB3 0HE, UK

(*Received 17 June 2000; accepted 27 September 2000*)

A new type of chiral smectic elastomer based on poly[4-(6-acryloyloxyhexyloxy)benzoic acid] is discussed. The layer structure and the molecular tilt stabilized by hydrogen bonding between side groups are identified by X-ray measurements. Well aligned and optically clear monodomain samples with smectic layers in the film plane are obtained by uniaxial stretching and then frozen-in by additional gamma-radiation crosslinking. In this monodomain state, two opposite orientations of director tilt are distributed through the sample thickness and alternate between neighbouring layers in a zigzag fashion. This structure of the stress-aligned chiral smectic C elastomer is similar to that of antiferroelectric liquid crystals of the smectic C$_A^*$ type. Further mechanical stretching in the layer plane induces a gradual *c*-director reorientation along the new stress axis, when a threshold deformation ~20% is exceeded. The (reversible) transition proceeds as a director azimuthal rotation around the smectic C cone, with the layers essentially undistorted and the tilt angle of the side mesogenic groups preserved.

1. Introduction

Liquid crystal (LC) elastomers represent a new group of materials having unusual structures and anisotropic behaviour, particularly as related to their mechanical properties [1–6]. In contrast to the extensive experimental investigations and theoretical studies of nematic poly- and mono-domain elastomers, less attention has been paid to the structure evolution and mechanical properties of smectic elastomers. Smectic polymer networks and particularly the chiral smectic C (SmC*) elastomers are of special interest, because they show important physical effects such as ferroelectricity, piezoelectricity, etc., if the helical superstructure is unwound. The mechanical properties of elastomers are of great importance in this context because the polymer elasticity, when coupled with the smectic C* order, may provide an efficient way of unwinding the helix and aligning the LC director through the influence of mechanical stretching [7, 8].

The main objective of this paper is to study the mechanism of the stress-induced director orientation and reorientation in chiral smectic elastomers. The special feature of our system is the fact that the liquid crystalline properties are provided and stabilized by hydrogen (H)-bonding. These materials enable a certain ease of control and manipulation of their properties by just adding different low molecular mass agents, which form pronounced mesogenic groups by H-bonding into rod-like complexes with the pendant moieties of the side group polymer. At the same time, such side group complexes have no strong influence on the network topology [9]. The main result reported here is the characteristic zigzag alignment of the LC director in the alternating layers of a chiral smectic C, similar to that in the

---

*Author for correspondence; e-mail: rtalroze@ips.ac.ru

Liquid Crystals ISSN 0267-8292 print/ISSN 1366-5855 online © 2001 Taylor & Francis Ltd
http://www.tandf.co.uk/journals
DOI: 10.1080/02678290010017953

antiferroelectric smectic C_A^* phase recently discovered and studied in low molar mass liquid crystals—see, for example, [10, 11].

We chose to place the chiral moieties into such low molecular mass agents. The side group polymer had a fairly typical acrylate structure leading to a tilted smectic C ordering after the H-bonded complexes are established. The scheme shows a typical structure, involving low molecular mass optically active 4-[*S*-(−)-2-methylheptyloxy]benzoic acid (O*OBA) and chemical crosslinking by interaction with 1,6-hexamethylene di-isocyanate (HMDI). O*OBA is structurally similar to the side group mesogenic cores of the H-bonded complex and this results in the formation of mixed chiral dimers attached to the polymer backbone, as shown in the scheme.

2. Experimental

The monomer, 4-(ω-propenoylhexyloxy)benzoic acid, was synthesized as previously described in [12]. The chains were formed by polymerization in benzene at 65°C for 35 h; 2,2′-azoisobutyronitrile (0.1% of the total weight of the monomer) was used as initiator. The polymer precipitated from the benzene solution during the polymerization. It was separated, dissolved in tetrahydrofuran (THF), reprecipitated with benzene and dried; yield 60%. After polymerization, 10 mol % of the low molecular mass optically active 4-[*S*-(−)-2-methylheptyloxy]benzoic acid (O*OBA) was added to provide the chiral power in the system.

Poly[4-(6-acryloyloxy-hexyloxy)benzoic acid] (PA-6BA) is a polymer exhibiting liquid crystalline properties [13]. It has a rather high glass transition temperature ($T_g = 100°C$) as well as a high clearing point ($T_c = 167°C$). The reason for the mesogenic order is thought to be the formation of cyclic dimers based on linking of the similar monomer units as shown in the scheme. The presence of stabilizing cyclic dimers by H-bonding of the carboxyl groups is proved by the presence of the band at 1680 cm^{-1} in the IR spectrum of the bulk polymer (figure 1, spectrum 1). This band is related to the stretching mode of the C=O bond in well established cyclic dimers [14, 15]. The C=O stretching of the ester linkage between the polymer backbone and the side group has a characteristic frequency at 1734 cm^{-1}. The band at 1608 cm^{-1} is characteristic of phenyl ring stretching. The band at 1580 cm^{-1} also appears to be due to the phenyl ring stretching, but as a result of conjugation of the ring with the electron accepting C=O group in the carboxyl group. The high frequency bands at 2500–3080 cm^{-1} are in the ν(C–H) stretching region.

The presence of cyclic dimers is also confirmed by the IR spectra for the chiral additive O*OBA, as well as for its blend with PA-6BA (figure 1, spectra 2 and 3, respectively). Both spectra contain similar major bands to those characteristic of the spectrum of PA-6BA, except for the one corresponding to the C=O stretch at 1734 cm^{-1}, which is absent from spectrum 2 because there is no COO ester group in the molecules of the chiral acid. The blend composed of 90 mol % of PA-6BA and 10 mol % of O*OBA (figure 1, spectrum 3) should consist of H-bonded homodimers like PA-6BA : PA-6BA (A in the scheme) and PA-6BA : O*OBA mixed dimers (B in the scheme); the homodimers O*OBA : O*OBA

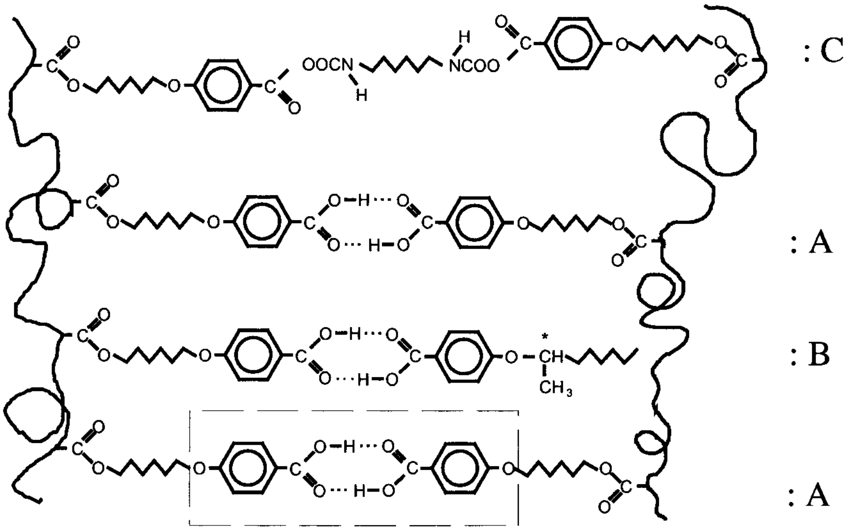

Scheme. Three main types of structural element within the polymer network: H-bonded rod-like dimers (A) formed by the carboxyl groups of the monomer units incorporated in the polymer backbone (shown schematically by the wavy line); mixed dimer (B) containing the H-bonded carboxyl unit formed by the chiral molecule O*OBA; and the crosslinking bridge (C) containing a 1,6-hexamethylene fragment.

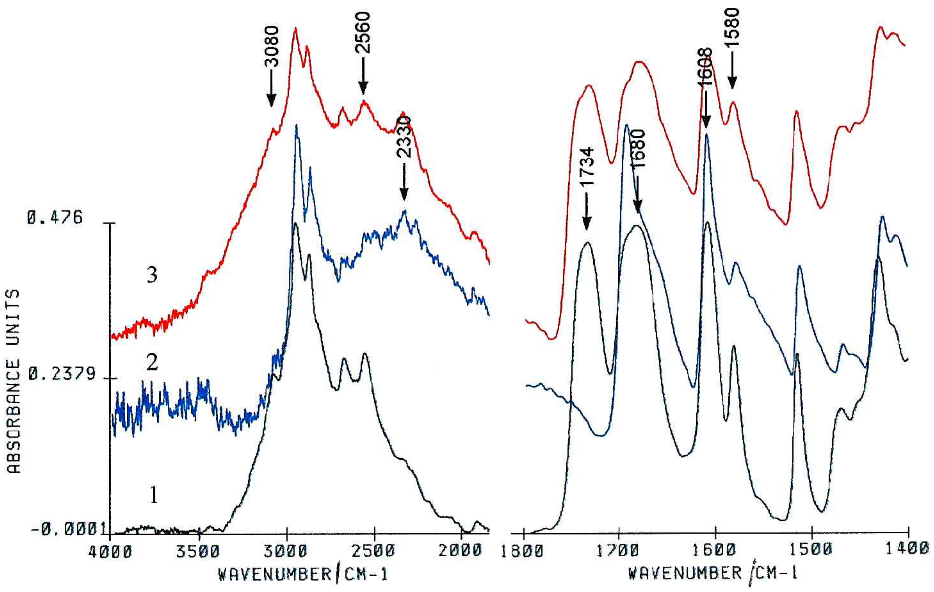

Figure 1. IR spectra of the polymer PA-6BA (curve 1), optically active additive O*OBA (curve 2) and their blend containing 10 mol % of O*OBA (curve 3) at room temperature.

may also be present, but in a much lower proportion. There is no direct evidence for the mixed dimers formed by individual components in the blend because of the overlap between the major spectral bands, but as was shown recently [16], the mixed dimer appears and often dominates the structure in mixtures of H-bonded acids.

Chemical crosslinking was carried out using a THF solution containing the linear polymer, O*OBA (10 mol %) and the crosslinking agent 1,6-hexamethylene di-isocyanate (HMDI, 5 mol %). After a homogeneous solution was obtained, the solvent was distilled off. The polymer blend with O*OBA and the crosslinking agent was dried in vacuum at room temperature. After complete removal of the solvent, the sample was placed in a temperature controlled chamber, where crosslinking proceeded for 1 h at 25°C.

In normal circumstances, a crosslinked network of a liquid crystalline polymer inevitably forms a polydomain texture with a relatively small length scale of the texture, of the order of ~1 μm [2]. Such a rapid variation of birefringence axis causes strong light scattering and makes the materials optically opaque. If a polydomain elastomer is uniaxially stretched, its director aligns and the material becomes optically transparent: a polydomain–monodomain transition occurs [6], an effect well studied in nematic and ordinary smectic elastomers. An established way to prepare a permanent monodomain director orientation in elastomers is to align them by mechanical stretching and then additionally crosslink them under stress to preserve the established alignment, [7]. In our case, polydomain samples were stretched by a large factor of the order ~2.5, and then quenched below the glass transition; the additional crosslinking was then performed by gamma-irradiation of the aligned glassy state. Polymer films were placed in ampoules, and evacuated for 1 h at room temperature at 0.133 Pa. The ampoules was then sealed and gamma-irradiated to the dose of 1 MGy at room temperature. The dose rate was 0.036 MGy h^{-1} (gamma-radiation from a ^{60}Co source); see [17] for further details of the method.

The phase behaviour of the systems under investigation was studied with a Mettler TA-4000 differential scanning calorimeter equipped with a DSC-30 heating cell. The DSC data were acquired at a heating rate of 10 K min^{-1}.

Wide angle X-ray scattering measurements were carried out using monochromatic CuK_α radiation and a two-dimensional image plate system (700 × 700 pixels, 250 μm resolution). The X-ray scattering experiments to obtain the temperature dependence of the structures were performed after annealing the samples for 30 min at the desired temperature. The direction of the incident beam was essential in this study. In order to analyse the structures unambiguously, we had to vary the inclination of the beam with respect to the sample plane from the 'traditional' incidence perpendicular to the surface to a very oblique angle nearly parallel to the elastomer film. Wide and small angle scattering patterns were also obtained using DRON-3.0 and IRIS-3.0 instruments (CuK_α radiation, Ni-filtered, transmission mode).

Stress–strain curves associated with orientational transitions occurring in the elastomer samples under deformation were obtained with a purpose-built tensile device described elsewhere [18]. The accurate measurement of very small changes in stress over large time intervals demanded that the experimental error be reduced to 0.05% in stress and 0.1 K in temperature. The measured load, in arbitrary units, was converted into nominal stress, σ, by calibration with weights and calculations based on the geometry of the samples. The extension is given in engineering strain format calculated from the applied extension and sample dimension, $\varepsilon = \Delta L/L_0$.

3. Results and discussion

Small angle X-ray diagrams given in figure 2 help in identifying the structure of the polymer before crosslinking. The maximum with the d_1-spacing equal to 2.88 nm (with the secondary peak at the effective $d_2 = 1.44$ nm), combined with the broad amorphous halo at wide angles, indicate the smectic-like order. The addition of 10 mol % of chiral units slightly decreases the clearing point of the system, to 156°C, but does not change the d-spacing (figure 2). This proves the similarity to the initial smectic-like polymer structure, although one may anticipate that the addition of the chiral additive transforms the phase into a chiral smectic phase. The chemical crosslinking with 5 mol % of HMDI, which acts additionally to stabilize the H-bonded layered microstructure, also does not significantly influence the d-spacing of the smectic layers (corresponding X-ray scattering images confirm this layer spacing of $d_1 = 2.88$ nm).

The chemically crosslinked elastomer has a polydomain texture and an opaque appearance due to the strong scattering of light by the spatially varying axis of optical anisotropy. On application of a uniaxial strain the sample becomes monodomain, with an optically transparent appearance. The analysis of azimuthal scans of the wide angle X-ray scattering pattern, changing from the amorphous halo to a well separated azimuthal distribution during the polydomain–monodomain transition, gives an idea of the degree of alignment of the mesogenic groups. Figures 3 (*a*-*c*) show examples of 360° azimuthal scans before, during and after the transition, respectively. Figure 4 presents the calculated orientational order parameter $S = \langle 1/2 \cos^2 \phi - 1/2 \rangle$, with ϕ the angle between the local optic axis and the stretching direction. One clearly identifies the threshold of the polydomain–monodomain transition and a sharp increase in $S(\varepsilon)$ above the threshold $\varepsilon_c \sim 0.45$. The data are fitted by the law $S \sim \exp[-m/(\varepsilon - \varepsilon_c)^{1/2}]$, cf. [6]. At a strain $\varepsilon > 60\%$, the orientational ordering effectively saturates at a value $S \approx 0.3$ and the elastomer film attains a uniformly

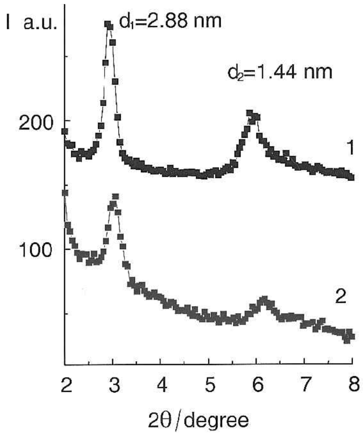

Figure 2. Small angle X-ray diffractograms of PA-6BA (curve 1) and its blend with 10 mol % O*OBA (curve 2) at room temperature.

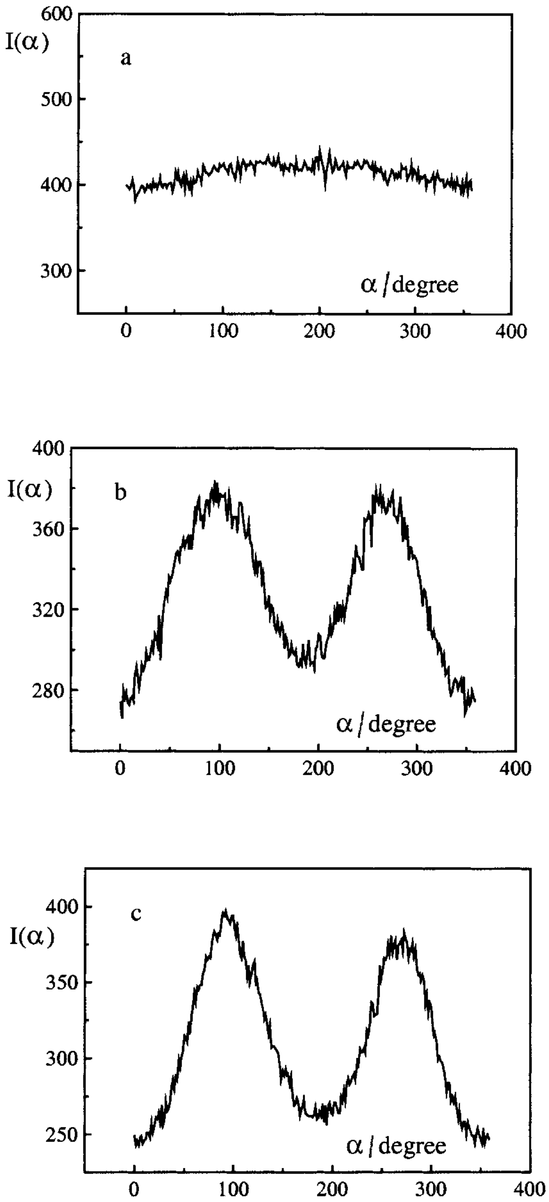

Figure 3. Strain dependence for the azimuthal wide angle X-ray scans showing the orientation of the mesogenic groups (*a*) before the polydomain–monodomain transition, (*b*) in the vicinity of the strain threshold $\varepsilon_c \sim 45\%$, and (*c*) at a large strain $\varepsilon \sim 80\%$; the latter shows a well aligned c-director.

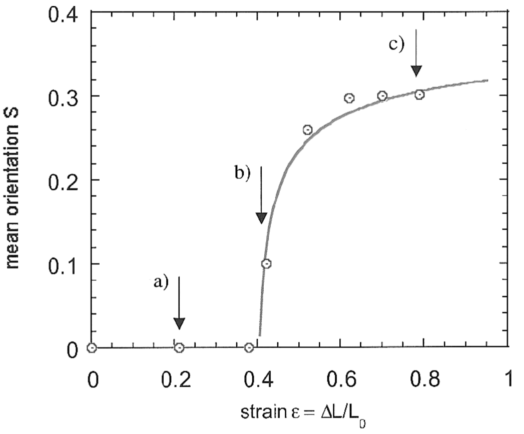

Figure 4. The mean orientation parameter S showing the degree of mesogenic group alignment along the stretching axis Z^0 as a function of strain applied at $T = 90°C$. The data, obtained from wide angle X-ray scattering scans, are fitted by a theoretical curve $S \sim 0.43 \exp[-0.14/(\varepsilon-\varepsilon_c)^{1/2}]$. The arrows on the plot show the points where the azimuthal scans of figure 3 are taken.

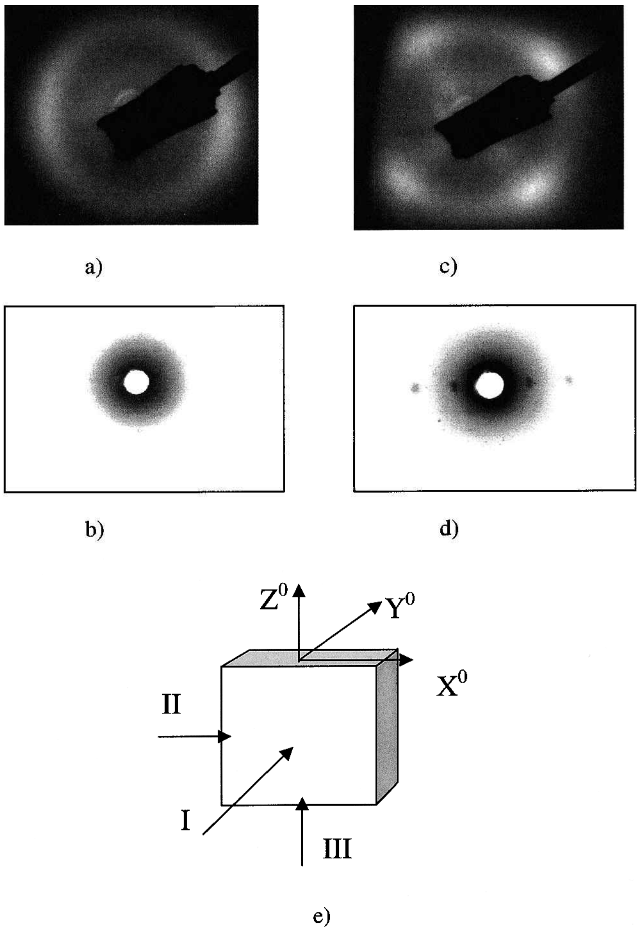

Figure 5. Wide angle (*a*, *c*) and small angle (*d*, *d*) X-ray diffraction patterns of the monodomain PA-6BA: O*OBA elastomer aligned in the Z^0 direction, measured in two different projections (see diagram, *e*) with the incident beam perpendicular (*a*, *b*) and parallel (*c*, *d*) to the Z^0X^0 film plane.

birefringent configuration with the principal axis along the stretching direction. The final value of S may appear rather low, especially if compared with a typical nematic order parameter $S \geqslant 0.6$. One must recall, however, that our material is a tilted smectic, and not a nematic liquid crystal. Indeed, we shall see shortly, from the analysis of small angle scattering in different orientations, that a smectic C tilted director microstructure is obtained in this system, with the layers aligned in the sample plane along the stretching direction. As a result, only the projections of the tilted mesogenic groups on the layer (and the sample) plane are oriented parallel to the stretching axis Z^0: this explains the low degree of apparent orientational order $S \approx 0.3$.

The overall microstructure of the monodomain elastomer, prepared according to the two-stage cross-linking with uniaxial stretching protocol, is quite different from that expected for 'classical' nematic or smectic liquid crystals. Figures 5 (*a*) and 5 (*b*) show the scattering patterns (at wide and small angles, respectively) for an X-ray beam directed perpendicular to the mechanically aligned monodomain sample film, which is in the Z^0X^0 plane, beam I in figure 5 (*e*).

From the wide angle pattern it is clear that the director is aligned along the axis of stretching, the vertical Z^0; the small angle pattern shows no layer reflections (we shall find that the smectic layers are aligned in the Z^0X^0 plane of the sample). Wide and small angle diffraction patterns for beam direction II, nearly in the sample plane, perpendicular to the stretching axis Z^0, are shown in figures 5 (*c*) and 5 (*d*), respectively. The small angle scattering pattern indicates a very good smectic layer alignment in the Z^0X^0 plane, with the same *d*-spacing as that determined from the powder averages in figure 2, $d = 2.88$ nm. The wide angle scattering pattern, figure 5 (*c*), is very interesting. It indicates that an almost equal number of mesogenic groups (formed by H-bonded cyclic dimers) is tilted with respect to the smectic layer normal in both directions in the Z^0Y^0 plane (the plane of stretching and the layer normal); the tilt angle is approximately 40°. This corresponds to a smectic C type of order, with the *c*-director changing by ~ 180° between consecutive layers or groups of a few layers. If we recall that the material is chiral due to a 10 mol % concentration of O*OBA integrated into the polymer structure, the analogy with the recently discovered antiferroelectric smectic C_A^* phase [10, 11] becomes very strong. We believe that a small asymmetry of the four wide angle maxima in figure 5 (*c*) is due to the small obliqueness of the X-ray beam (it was difficult for us to direct the beam exactly in the plane of the thin flat sample); however, it is possible that there is an additional effect of a small azimuthal deviation, 180° ± δ also found in antiferroelectric smectic C_A^* materials due to chirality [10, 11]. Ignoring this possibility for the moment, a schematic representation of the zigzag antiferroelectric molecular orientation leading to these X-ray patterns is given in figure 6 (*a*).

The orientation of the film described above was fixed within the elastomer by randomly adding crosslinks formed under the gamma irradiation. We now study the process of director reorientation under the application of mechanical stress in the Z^0X^0 plane along the X^0 axis, perpendicular to the initial stretching direction Z^0. Figure 6 (*b*) shows a sketch of the newly stretched sample and the resulting molecular arrangement, with the model X-ray scattering patterns in the three principal directions of beam incidence. The stress response during the stretching of the monodomain elastomer film in the Z^0X^0 plane, along the X^0 axis is given in figure 7. The strain rate of imposed deformation was kept constant and relatively low ($4 \times 10^{-5}\ \mathrm{s}^{-1}$) to ensure sufficient mechanical equilibration (see [18] for a discussion of slow stress relaxation). One can see that the stress–strain curve consists of two parts, again indicating a threshold behaviour. In the first regime, at deformations below 20%, the linear stress–strain variation gives an estimate of the elastic modulus for stretching in the layer plane perpendicular to the *c*-director alignment. This modulus, $G \approx 1.27$ MPa, has a value common for a rubbery polymer network. An abrupt change of stress–strain slope occurs at a threshold deformation of ~20%, when the elastic modulus takes a much lower value, $G \approx 0.32$ MPa. The X-ray diffraction patterns of the sample just above the threshold deformation ($\varepsilon \geqslant 20\%$) are given in figure 8. There is a broadening and eventual joining of arcs for the beam incidence I perpendicular to the sample plane,

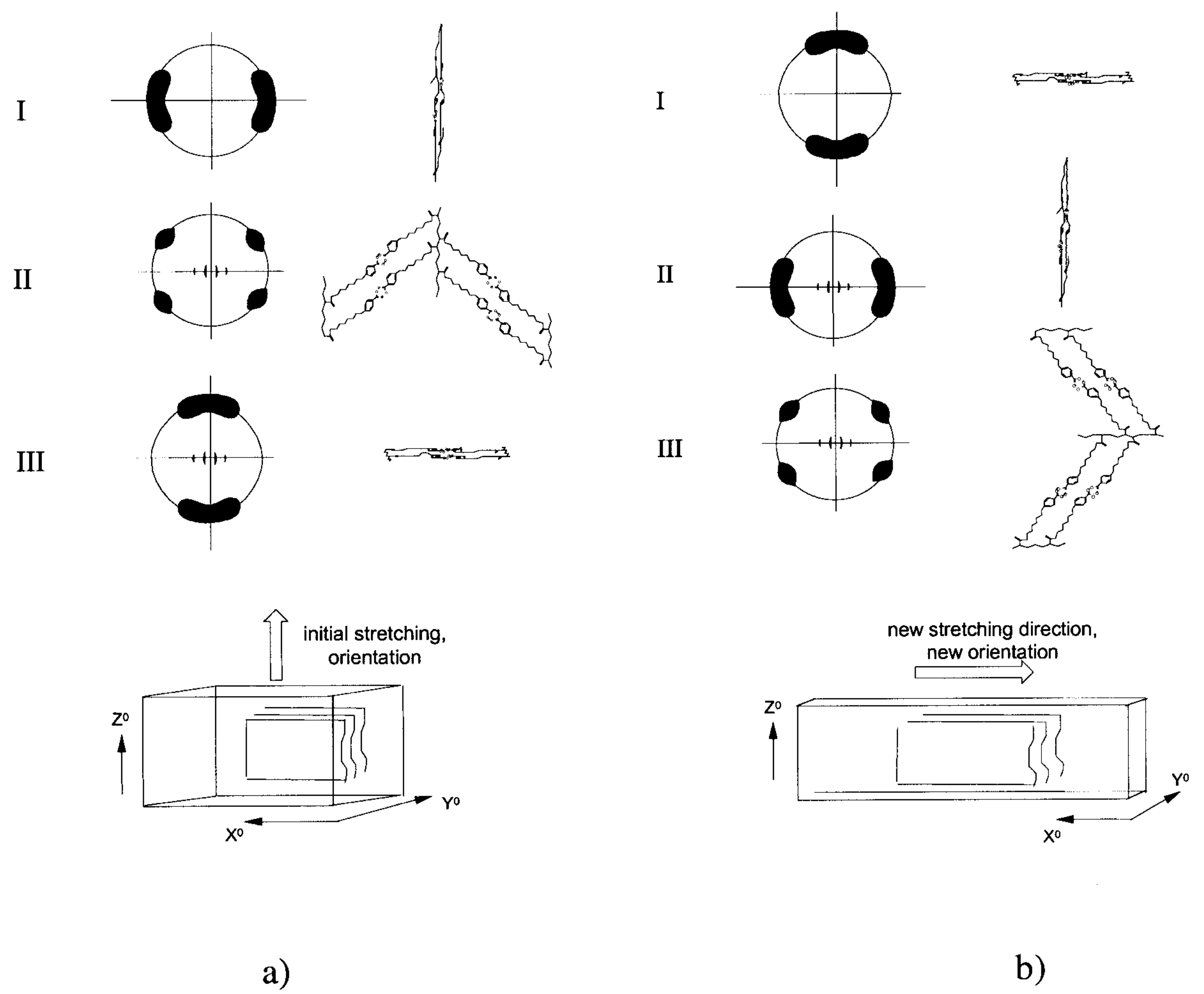

Figure 6. Schemes for the molecular structure in projection and model X-ray patterns observed in the corresponding geometries, with the beam directed towards the Z^0X^0 (I), Z^0Y^0 (II) and X^0Y^0 (III) planes. The diagrams (*a*) show the structure of the stress-aligned monodomain sample, diagrams (*b*) show how this orientation is changed after a perpendicular stress is applied in the X^0 direction.

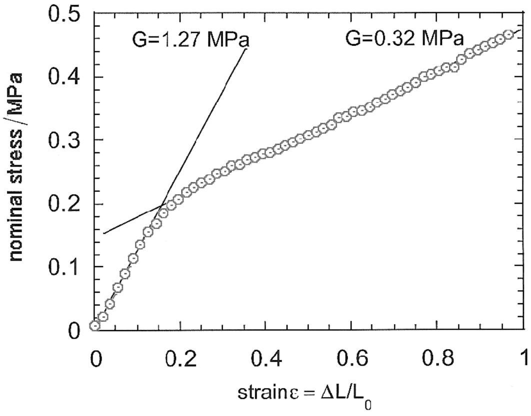

Figure 7. Stress–strain curve obtained on stretching and reorientation of the monodomain elastomer in the direction perpendicular to the initial orientation, at $T = 90°C$. Two distinctly different slopes are obtained before and after the threshold strain, giving the effective modulus changing from ~1.3 to ~0.3 Mpa.

figure 8 (*a*), and a broadening of the four-spot pattern for the beam II in the sample plane along the new stretching direction, figure 8 (*b*). At the same time the layered structure is still preserved, as shown by the small angle X-ray pattern, figure 8 (*c*).

We thus conclude that the mechanically induced orientational transition proceeds with undisturbed smectic layers and reorientation of the *c*-director alignment from the Z^0 axis to X^0, as schematically drawn in figure 6. The texture distortion is localized primarily in the layer plane and is characterized, in the vicinity of the threshold transition, by disordering (or twisting) of the *c*-director. At the same time the continuing presence of the four fold symmetry picture shows that the orientation of the side mesogenic groups is still preserved at an essentially unchanged tilt angle to the layer plane. The gradual realignment of the *c*-director in undistorted parallel smectic layers along the new stretching axis X^0 proceeds above the threshold strain, along the second region of the stress–strain curve. The mechanical and the X-ray structural evidence indicate that the alignment is continuously improved with strain increase and at about 100% strain, the resultant orientational order parameter S approaches the initial value of $S \approx 0.3$ (cf. figure 4).

4. Conclusion

We have prepared a new type of chiral smectic elastomer where the layer structure and the molecular tilt are stabilized by H-bonding between side groups. The two-stage crosslinking protocol, with intermediate uniaxial stretching, results in well aligned and optically clear monodomain samples with smectic layers in the film plane. X-ray study of the molecular orientation in this monodomain smectic state reveals an unusual tilted director structure with ~180° alternating tilt direction between the layers. The four-arc symmetry of X-ray scattering at wide angles indicates that both directions of molecular tilt are equally represented. On the one hand, this molecular alignment might be expected because the uniaxial extension does not have a particular direction, so that the mesogenic moieties may equally tilt both ways along the Z^0 axis. On the other hand, if we were to assume the smectic C structure with flat undistorted layers, the two orientations of tilt represented in the sample would result in a domain structure in the sample plane and domain walls between regions with different tilt directions, say, 0° and 180°. We do not see this at all in our uniform and optically transparent samples. We, therefore, are drawn to the conclusion that two opposite orientations of tilt are distributed through the sample thickness (along the layer normal) and alternate between neighbouring layers (or possibly groups of a very few layers) in a zigzag way. In this case, the observed optical uniformity would be consistent with the combination of X-ray data. This proposed structure of the stress-aligned elastomer is remarkably similar to the structure of antiferroelectric liquid crystals of the smectic C$^*_A$ type.

This work was supported by the INTAS under Grant #96-1401 and by the Russian Foundation of Basic Research (Grant No. 99-03-33411a). We are grateful to

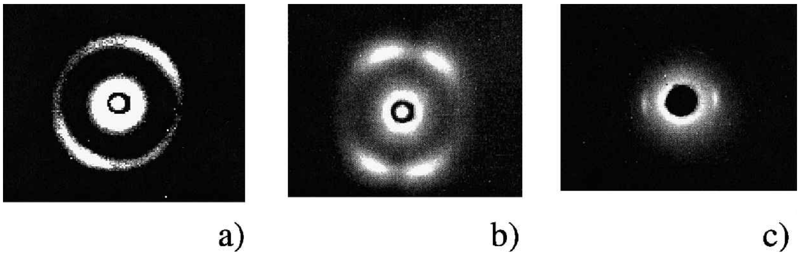

Figure 8. Wide (*a*, *b*) and small (*c*) angle X-ray diffraction patterns of the monodomain PA-6BA: O*OBA elastomer, initially aligned along Z^0, stretched up to $\varepsilon \sim 20\%$ along X^0 (just above the transition threshold seen in figure 7), measured in two different projections: perpendicular (*a*) and parallel (*b*, *c*) to the Z^0X^0 sample plane. One can identify the director rotation in the sample plane (*a*) and the unchanging zigzag layer alignment (*b*, *c*).

Prof. H. Finkelmann and Dr S. M. Clarke for numerous and useful discussions and support.

References

[1] Kundler, I., and Finkelmann, H., 1995, *Macromol. Chem., rapid Commun.*, **16,** 679; Kundler, I., and Finkelmann, H., 1998, *Macromol. Chem. Phys.*, **199,** 677.

[2] Clarke, S. M., Terentjev, E. M., Kundler, I., and Finkelmann, H., 1998, *Macromolecules*, **31,** 4862.

[3] Mitchell, G. R., Davis, F. J., and Guo, W., 1993, *Phys. Rev. Lett.*, **71,** 2947.

[4] Zubarev, E. R., Talroze, R. V., Yuranova, T. I., Plate', N. A., and Finkelmann, H., 1998, *Macromolecules*, **31,** 3566.

[5] Zubarev, E. R., Talroze, R. V., Kuptsov, S. A., Merekalov, A. S., Yuranova, T. I., Plane, N. A., and Finkelmann, H., 1999, *Liq. Cryst.*, **26,** 1531.

[6] Fridrikh, S. V., and Terentjev, E. M., 1999, *Phys. Rev. E*, **60,** 1847.

[7] Benne, I., Semmler, K., and Finkelmann, H., 1995, *Macromolecules*, **28,** 1854.

[8] Zentel, R., Reckert, G., Bualek, S., and Kapitza, H., 1989, *Macromol. Chem.*, **190,** 2869.

[9] Kato, T., 1998, *Handbook of Liquid Crystals*, Vol. 2B, edited by D. Demus, J. Goodby, G. W. Gray, H.-W. Spiess and V. Vill (Weinheim: Wiley-VCH), p. 969.

[10] Takezoe, H., Lee, J., and Chandanani, A. D. L., 1991, *Ferroelectrics*, **144,** 187.

[11] Mery, S., Lotzsch, D., Heppke, G., and Shashidhar, R., 1997, *Liq. Cryst.*, **23,** 629.

[12] Portugall, M., Ringsdorf, H., and Zentel, R., 1982, *Makromol. Chem.*, **183,** 2311.

[13] Shandryuk, G. A., Koval', M. A., Kuptsov, A. A., Bezborodov, V. S., Sosnovskii, G. N., Talroze, R. V., and Plate', N. A., *Polymer Sci.* (to be published).

[14] Azima, A., Brown, C. W., and Mitra, S. S., 1995, *Spectrochim. Acta*, **31A,** 1475.

[15] Bellamy, L. J., 1968, *Advances in Infrared Group Frequencies* (Bungay, Suffolk, Methuen).

[16] Kang, S. K., and Samulski, E. T., 2000, *Liq. Cryst.*, **27,** 377.

[17] Zubarev, E. R., Talroze, R. V., and Plate', N. A., 1999, *Polym. Sci.*, **26,** 1531.

[18] Clarke, S. M., and Terentjev, E. M., 1999, *Faraday Discuss.*, **112,** 325.